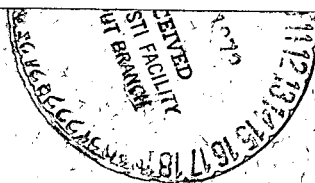


PHOTOELECTRON ESCAPE FLUXES OVER THE EQUATORIAL AND MIDLATITUDE REGIONS¹

(NASA-TM-X-68921) PHOTOELECTRON ESCAPE
FLUXES OVER THE EQUATORIAL AND
MIDLATITUDE REGIONS (NASA) 20 p HC
\$3.00

N73-16416

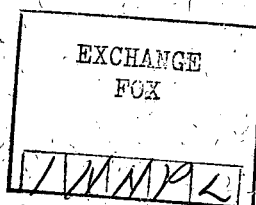
CSCL 04A

Unclas
G3/13 53100

B.C. Narasinga Rao

Risal Singh

E.J. Maier



JUNE 1972



RADIO SCIENCE DIVISION

NATIONAL PHYSICAL LABORATORY,
NEW DELHI-12, INDIA

RSD-75

RADIO SCIENCE DIVISION

Scientific Report No. 75

PHOTOELECTRON ESCAPE FLUXES OVER THE
EQUATORIAL AND MIDLATITUDE REGIONS¹

By

B.C.Narasinga Rao, Risal Singh

and

E.J. Maier²

June 1972

Approved by : *[Signature]*
Scientist-in-Charge, Radio Science Division

NATIONAL PHYSICAL LABORATORY, NEW DELHI - 12, INDIA.

-
1. To be published in the Indian Journal of Radio and Space Physics.
 2. NASA - Goddard Space Flight Center, Greenbelt, Md. USA.

CONTENTS

	Page
Abstract	1
1. Introduction	1
2. Measurement technique	2
3. Results	3
References	16

ABSTRACT

Satellite measurements of photoelectron escape flux around noontime made by Explorer -31 in 600-800 km altitude range are reported for the equatorial and midlatitude regions. The pitch angle distributions and the spectral distributions are derived from the data. The analysed data show that the flux for equatorial region is lower by a factor 2 to 3 in comparison to that of midlatitude region. Theoretical calculations are also made to compare with the observed escape fluxes.

1. INTRODUCTION

The photoelectrons produced in the ionosphere above about 300 km altitude can escape along the geomagnetic field lines as suggested by Hanson (1963). Indirect and direct evidences have been reported for the existence of photoelectron escape flux (Cole, 1965; Carlson, 1966; Rao and Donley, 1969; Rao and Maier, 1970; Heikkila, 1970). Theoretical investigations on the production and escape of photoelectrons were made by a number of workers notably by Nisbet (1968) and Nagy and Banks (1970). As the photoelectrons serve as the heat source to the ionospheric plasma both in the F-region and topside ionosphere, it is important to know the pitch angle distribution and also the spectral distribution for estimating heat inputs. These distributions are reported earlier by Rao and Maier (1970) in the topside ionosphere for sunrise conditions from direct measurements with retarding potential analysers aboard Explorer-31. The photoelectron flux for high latitudes has also been reported by Maier and Rao (1970) recorded by the same probe. There is a need to know the daytime photoelectron escape flux and their pitch angle and spectral distributions for low latitudes.

Theoretical studies (Shawhan and Block, 1970) have shown that the photoelectron flux reaches steady equilibrium values from about 0800 hrs to 1600 hrs. Therefore, any observations available during the above period may be utilized to represent the daytime distributions. This point is also tested from the observations.

The purpose of the present paper is to present further observations recorded by the Explorer-31 probe relating to midday photoelectron flux and their pitch angle and spectral distributions for equatorial latitudes around noontime in the 600-800 km region and compare them with those of midlatitudes.

2. MEASUREMENT TECHNIQUE

Measurements were made with a retarding potential analyser aboard Explorer-31. The details of the experiment have been described by Maier (1969) and Rao & Maier (1971). Integral fluxes above the thresholds of 3.7, 7.0, 11.0, 15.0 and 34.0 eV energy were available from the probe measurements. Differential energy spectra are derived from these values. Due to the spin of the satellite the sensor normal scans a wide range of angles with respect to the geomagnetic field. However, due to the direct incidence of the sun's rays on the sensor during part of satellite

rotation, flux measurements are not available for all angles because when the sun is illuminating the sensor the recorded flux will also include the electrons produced by ionisation within the sensor and hence the observed flux will not be the real ambient flux. The flux values presented in the results are only for the conditions in which sun is not incident on the sensor. For example during noon time at mid-latitudes useful measurements can be obtained when the sensor is looking towards the earth, which means that the flux refers to the upgoing (escaping) photoelectrons. Over the equatorial latitudes where the geomagnetic field lines are horizontal useful measurements can be obtained for fluxes moving in both directions. The following data are selected from observations made during Dec. 1965 to March 1966. Because the sensor aperture subtends a solid angle of about 2 steradians and receives the fluxes from the directions other than the one in which the sensor normal is pointing, it should be noted that the pitch angle distributions shown in the following results are average distributions and not the precise ones.

3. RESULTS

Fig. 1 shows the variation of integral flux ($E > 5$ eV) with solar zenith angle (χ) at 300 km base of the geomagnetic field line passing through the satellite location.

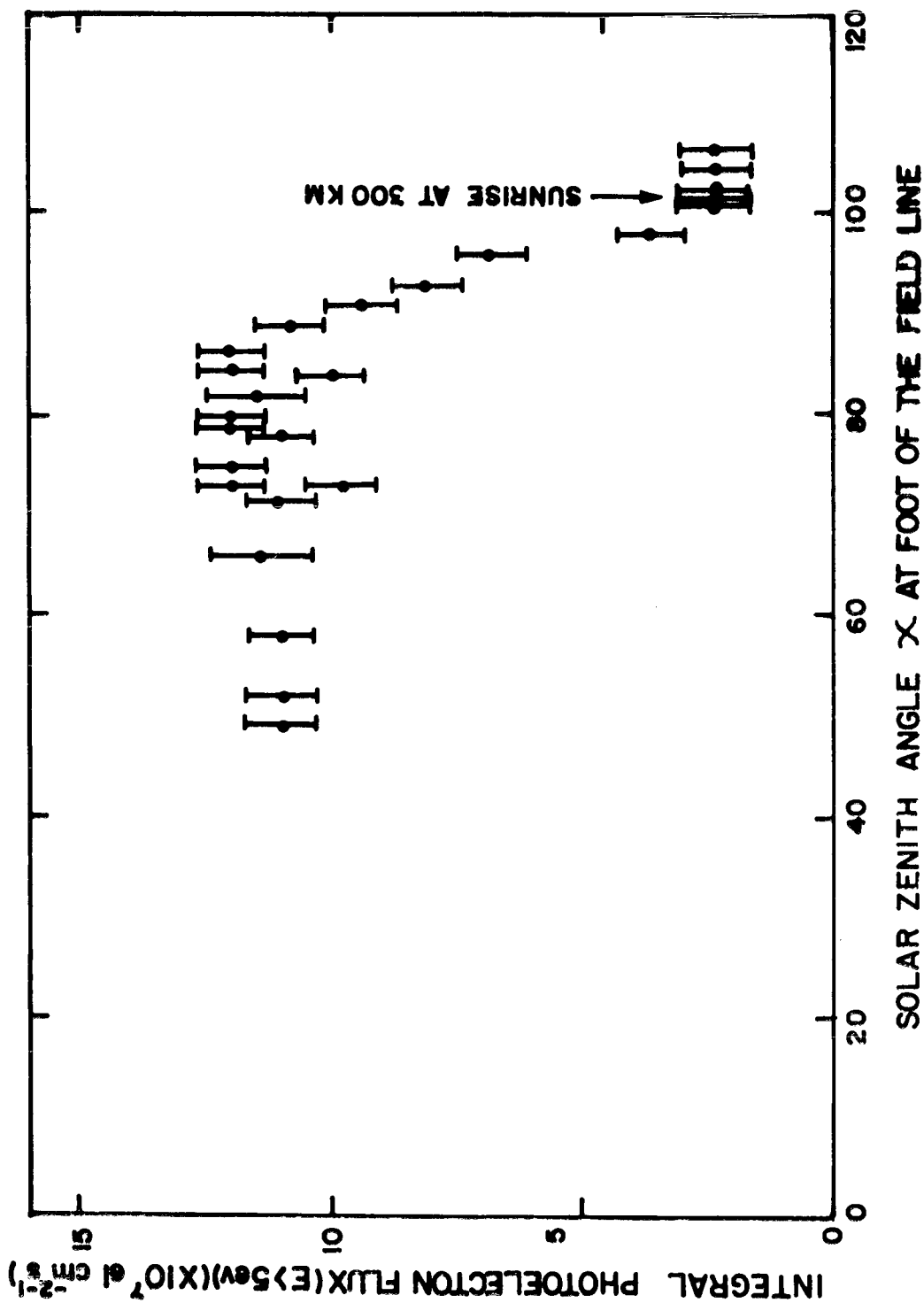


Fig. 1 Variation of integral photoelectron flux ($E > 5 \text{ eV}$) with solar zenith angle (χ) at 300 km base of the geomagnetic field line passing through the satellite location. The solar zenith angle at sunrise at 300 km is also indicated.

The solar zenith angle at sunrise at 300 km is also indicated in this Fig. The flux observed at the satellite position can be taken as the flux escaping from the ionosphere along the magnetic field line at the same time at which the observations at the satellite position are taken, because the photoelectrons take a few seconds to travel from one hemisphere along the field line to the other hemisphere. (The 10 eV electron takes only about 8 seconds to travel from one hemisphere along $L = 2$ field line to the other hemisphere). It is clear from the Fig. (1) that the background suprathermal flux ($E > 5$ eV) is nearly constant before sunrise ($1.2 \times 10^7 \text{ el cm}^{-2} \text{ sec}^{-1}$). As soon as the sun's rays appear at the 300 km level the flux increases rapidly and reaches a maximum value of about $1.2 \times 10^8 \text{ el cm}^{-2} \text{ sec}^{-1}$ within a very short period. After this the flux value remains nearly constant during the daytime. This shows that the flux attains a steady equilibrium value within an hour or so just after sunrise.

We have observed a decrease of flux over the equatorial region. Fig. 2 shows the observed integral photoelectron fluxes at two location of a satellite pass taken on Feb. 13, 1966 between 1200-1230 hrs of local time within the altitude range of 510 to 530 km. The first distribution depicted by thick points is at the magnetic

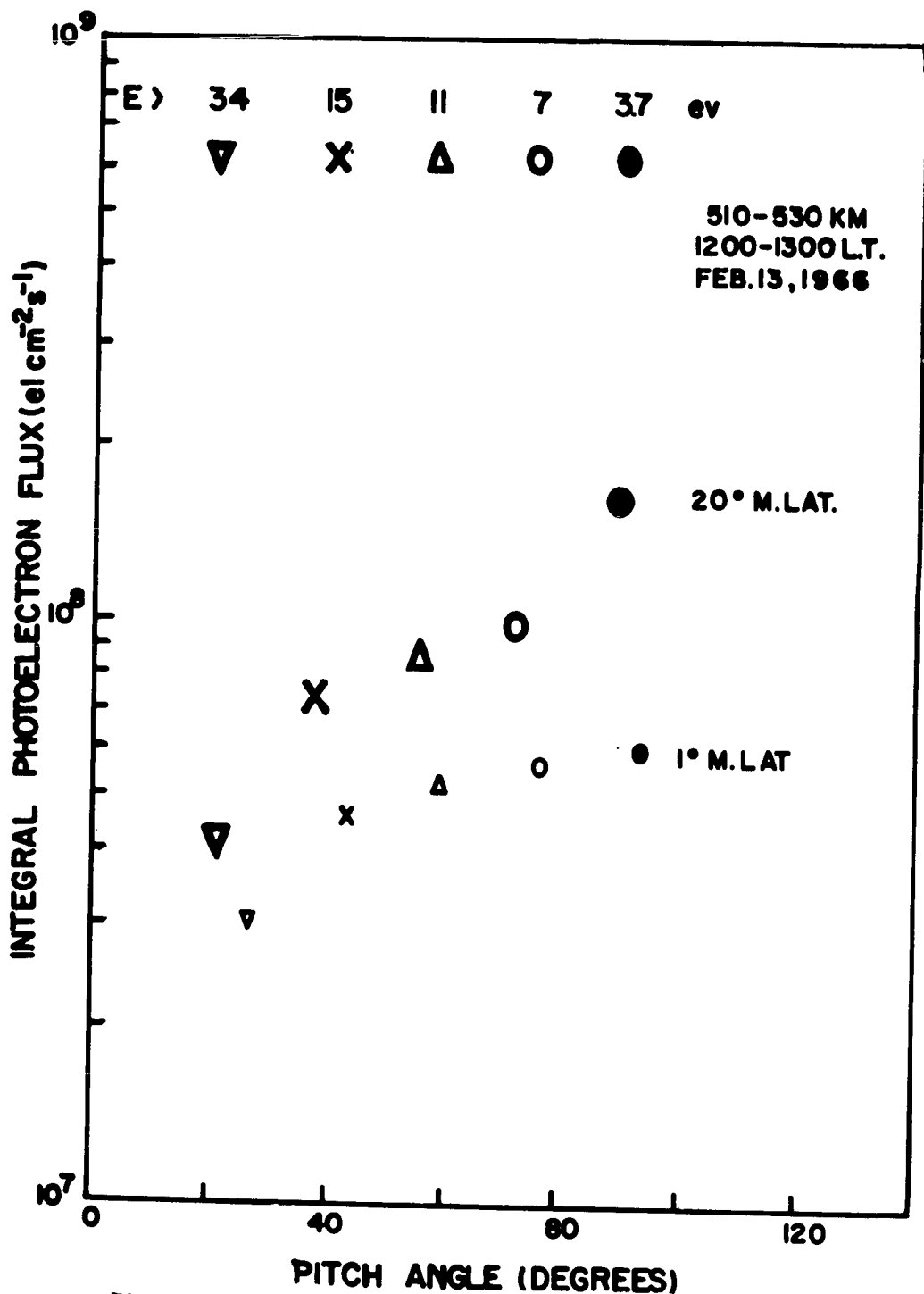


Fig.2 Observed integral photoelectron fluxes for different threshold energies at two locations of a satellite pass. The distributions depicted by thick and thin points are at magnetic latitudes of 1° and 20° respectively. Note that the pitch angles at the two locations are almost same for any particular threshold energy.

latitude 1° and the second distribution shown by thin points is for the magnetic latitude of 20° . This particular pass of the satellite is selected such that the altitude and the local time of the observations at two different magnetic latitudes are nearly the same. The pitch angle for the observations corresponding to every threshold energy is nearly same for both locations. As is evident from the Fig. the fluxes are lower in the equatorial region (1° Magnetic latitude) in comparison to those of the midlatitude region (20° Magnetic latitude). The ratio between the fluxes at these two latitudes is lowest (1:1.4) for the photoelectrons having energy equal to or greater than 34 eV, increases for those of lower energy and finally becomes maximum (1:2.5) for the photoelectrons having energy equal to or greater than 3.7 eV.

Fig.3 shows the pitch angle distribution of integral photoelectron flux for electrons having energies greater than 3.7, 7, 11 and 15 eV in the equatorial region. The energy levels listed are the retarding potentials with respect to the vehicle and are not corrected for vehicle potentials. By grouping several minutes of data we are able to obtain fairly complete coverage of angular distribution as shown in Fig.3. This pass of the satellite is chosen in the equatorial region for which magnetic latitude starts at 10.5°N and ends at 3°S .

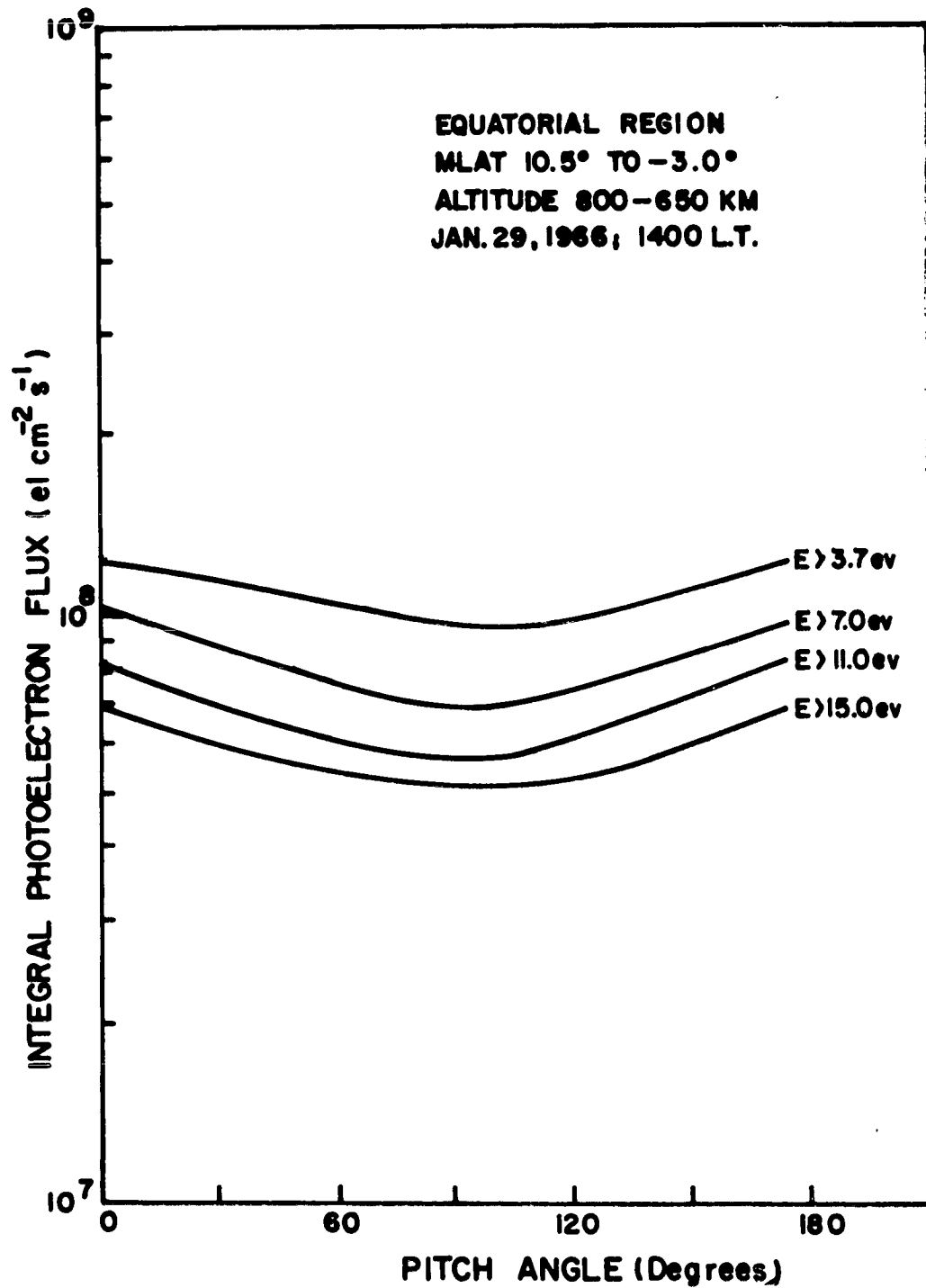


Fig.3 Pitch angle distribution of integral photoelectron flux for electrons having different threshold energies in the equatorial region.

As we have referred earlier, we can obtain good results only when the sun is not shining into the sensor. For observations taken where the solar zenith angle is very small (as in the present case which is taken at 1400 hrs of local time), useful data can be obtained for the directions of the sensor normals looking towards the earth. In the case of equatorial latitudes (as shown in Fig.3) the magnetic field lines are horizontal and the sensor normal covers 0 to 180° with respect to the field line. So, for this region, we can have the pitch angle distributions for all angles from 0 to 180° with respect to the field line. Thus in Fig.3 the pitch angle distributions for the photoelectron flux in the equatorial region is shown for all angles. The pitch angle distributions in Fig.3 show a minimum at 90° and a maximum at 0° or at 180° for all thresholds of energies.

Fig. 4 shows the pitch angle distributions of the integral photoelectron fluxes in the midlatitude region. This pass of the satellite covers the magnetic latitude from 31°S to 47°S and is taken at 1330 hrs of local time on Feb.6, 1966. The observations of pitch angle distribution cover an angular range from 90° to 180° only with respect to magnetic field line. This Fig. also shows that the pitch angle distribution has its minimum at 90° and maximum at 180° with respect to the field line, which corresponds to upward direction of flux motion along the field line.

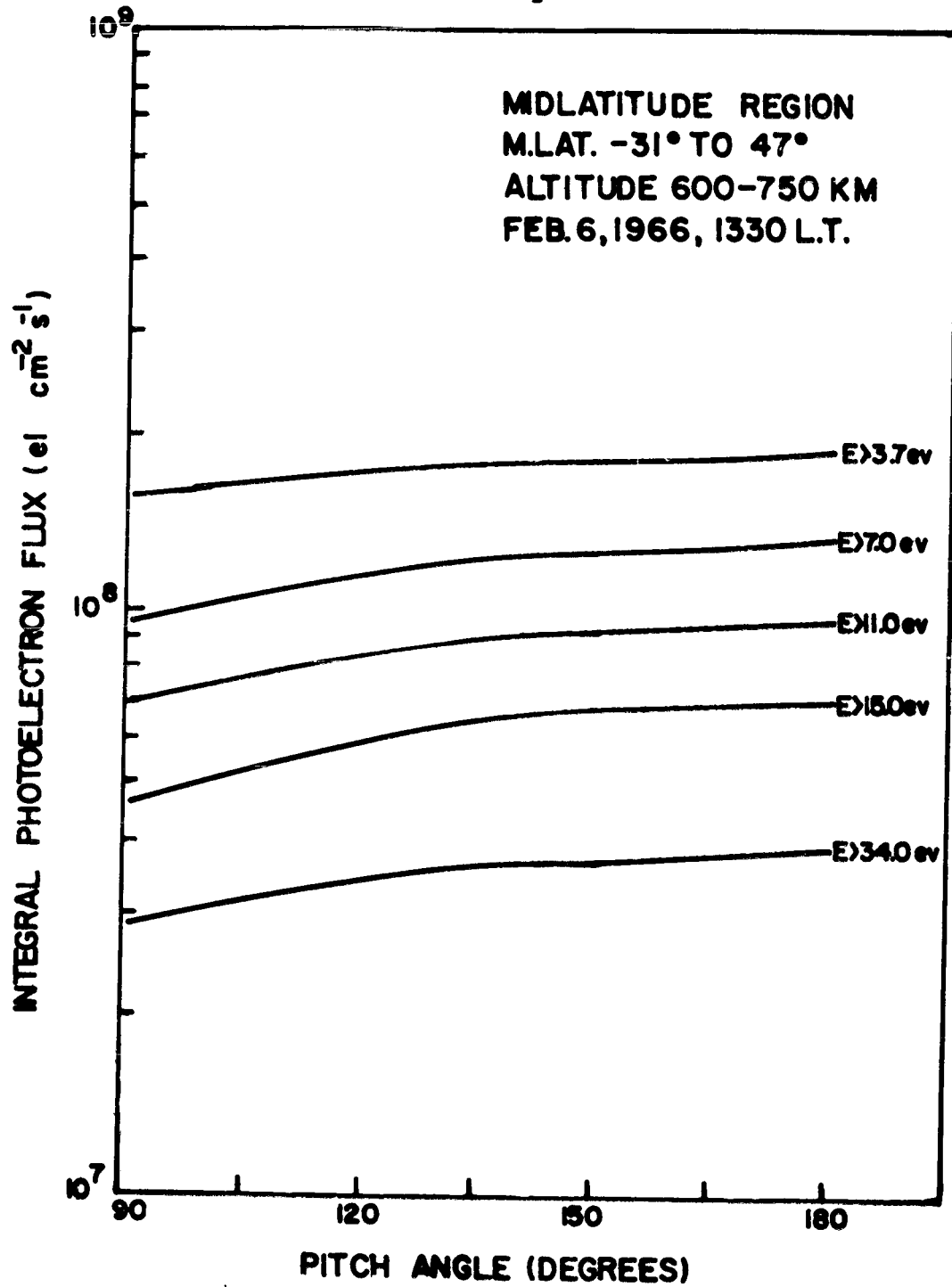


Fig.4 Pitch angle distribution of integral photoelectron fluxes for electrons having different threshold energies in the midlatitude region.

Fig.5 shows the spectral distribution of the photoelectron fluxes derived from the results of Figs.3 and 4 for 0° and 90° pitch angles. The spectral distribution indicates that the fluxes at low latitudes are lower than those for the midlatitudes by a factor of 2 for 0° for all energies and by a factor of 2, 3 and 4 for 90° for 5, 9 and 12 eV.

We have theoretically calculated the escape fluxes for equatorial and midlatitude regions following the procedure given by Nisbet (1968). The escaping flux is dependant on the magnetic dip and is given by

$$\phi_E = \int_V n_E v_E \sum_m n_m \sigma_{em} \exp(-\sum_m n_m \sigma_{em} H_m / \cos \alpha \sin I) dz$$

where n_E and v_E are the number density and velocity of the photoelectrons and m represents the m th constituent of the neutral atmosphere, σ_{em} is the total elastic cross-section, α is the pitch angle and I is the dip.

The photoelectron densities are scaled from the values given by Nisbet (1968) to correspond to noontime solar minimum conditions. The neutral atmospheric densities are taken from CIRA (1965) model for $F = 75$ units. The total elastic cross-sections for different species of neutral atmosphere (i.e. O , O_2 , N_2) are taken from Nagy and Banks (1970). The average $\cos \alpha$ value is taken as $3/8$.

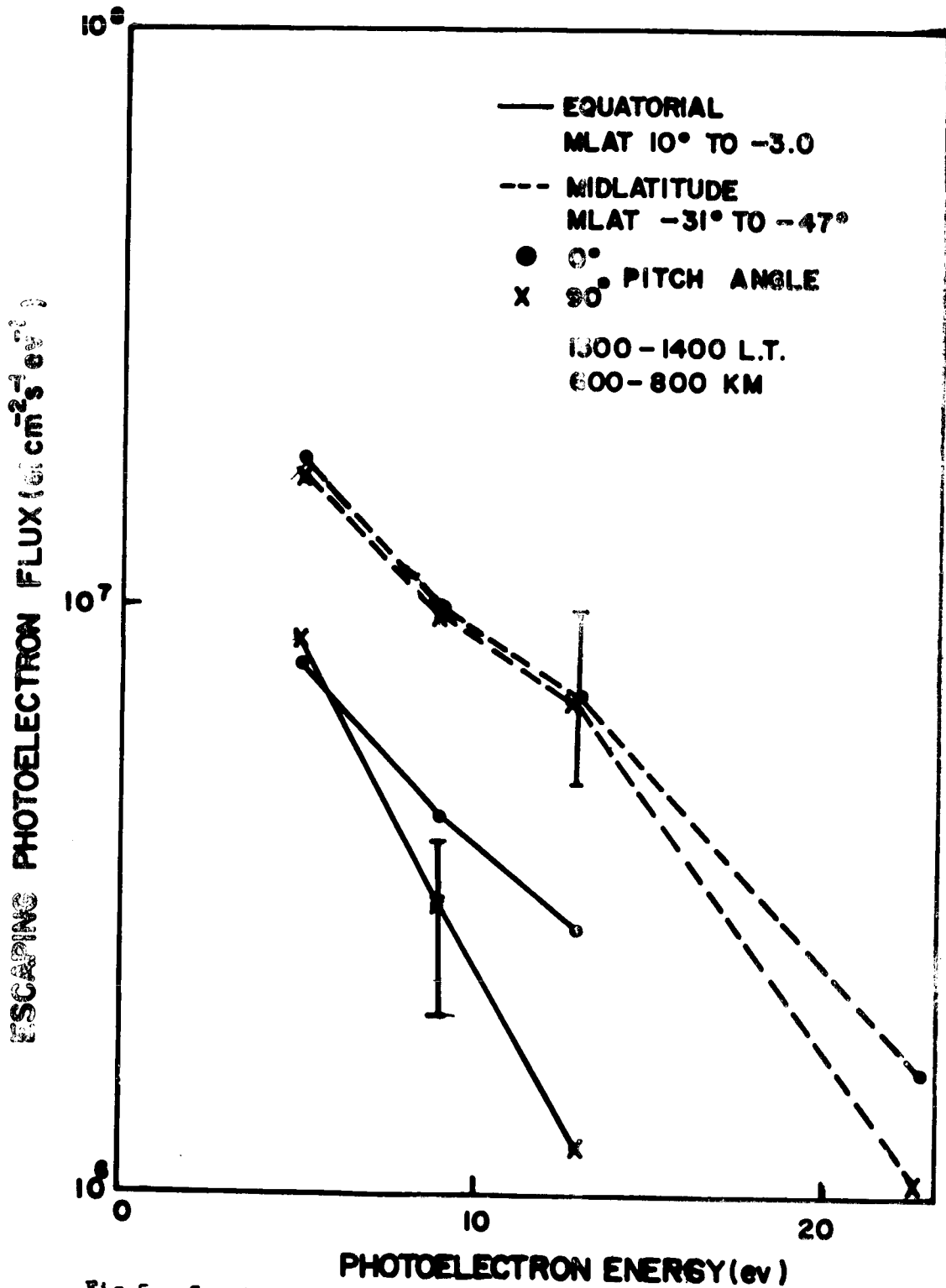


Fig.5 Spectral distributions of photoelectron fluxes for equatorial and midlatitudes derived from the results of Figs.3 and 4 for 0° and 90° pitch angles.

In the present case, escape fluxes are calculated for dip $I = 20^\circ$ and 50° (10° and 30° Mag. latitude) to represent equatorial and midlatitude regions. The field lines passing over the equator at altitudes of about 600 km reach down to 400 km at about 10° Mag. latitude. As most of the escape flux originates below 400 km level, the equatorial measurements roughly correspond to the escape fluxes over 10° Mag. latitude.

Fig.6 shows the variation of escape fluxes with altitude for photoelectrons of energy 5, 10 and 15 eV. It is clear from the diagram that the fluxes have become nearly constant with altitude at 500 km. We may compare these theoretical values with the experimentally observed data with regard to their absolute values as well as their ratios. The calculated fluxes are found to be larger than the observed in both the regions. This difference may be due to adapted values for photoelectron densities and neutral atmosphere densities. However, the ratios of the fluxes between these two latitudes should not be effected by these assumed models. It is seen from Fig.6 that the ratio between the fluxes at 20° and 50° of dip angles is 1:5. This ratio becomes slightly more if the scattering of photoelectrons is included on the lines suggested by Banks and Nagy (1970). It thus appears

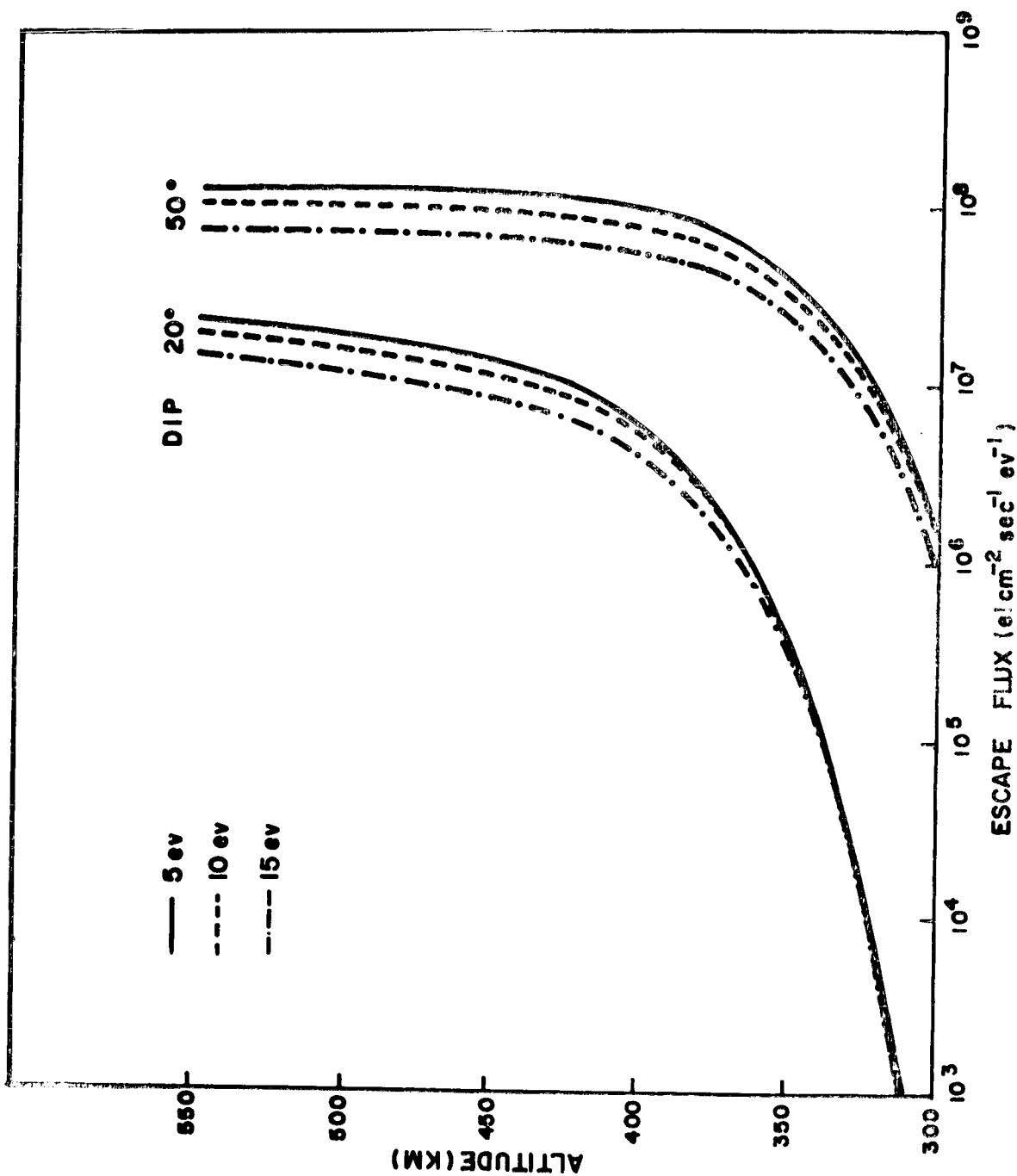


Fig. 6 Variation of escape fluxes with altitude for photoelectrons of energy 5, 10 and 15 eV at dip angles of 20° and 50° representing the equatorial and midlatitude escape fluxes.

that the theoretical estimates predict a decrease in escape flux in the equatorial region by a factor of 5 compared to midlatitudes while the observations show only a factor of 2 to 3 decrease. It is possible that the theory does not take into account all the operating mechanisms involved in the photoelectron escape flux. It is likely that electric fields in the ionosphere are important and that diffusion across the field lines may take place so that differences in fluxes with latitude may be reduced.

REFERENCES

- | | | |
|----------------------------------|------|---|
| BANKS, P.M. and NAGY, A.F. | 1970 | J. Geophys. Res., <u>75</u> , 1902. |
| CARLSON, H.C. | 1966 | J. Geophys. Res., <u>71</u> , 195. |
| COLE, K.D. | 1965 | Ann. Geophys., <u>21</u> , 156. |
| HANSON, W.B. | 1963 | Space Res., <u>3</u> , 282. |
| HEIKKILA, W.J. | 1970 | J. Geophys. Res., <u>75</u> , 4877. |
| MAIER, E.J.R. | 1969 | Proc. IEEE, <u>57</u> , 1068. |
| MAIER, E.J.R. and
RAO, B.C.N. | 1970 | J. Geophys. Res., <u>75</u> , 7168. |
| NAGY, A.F. and
BANKS, P.M. | 1970 | J. Geophys. Res., <u>75</u> , 6260. |
| NISBET, J.S. | 1968 | J. Atms. Terr. Phys., <u>30</u> ,
1257. |
| RAO, B.C.N. and
DONLEY, J.L. | 1969 | J. Geophys. Res., <u>74</u> , 1715. |
| RAO, B.C.N. and
MAIER, E.J.R. | 1970 | J. Geophys. Res., <u>75</u> , 816. |
| SHAWHAN, S.D. and
BLOCK, L.P. | 1970 | J. Atmos. Terr. Phys., <u>32</u> ,
1885. |